

Article

# Application of Bioelectrochemical System and Magnetite Nanoparticles on the Anaerobic Digestion of Sewage Sludge: Effect of Electrode Configuration

Nhlanganiso Ivan Madondo <sup>1,\*</sup> , Emmanuel Kweinor Tetteh <sup>1</sup> , Sudesh Rathilal <sup>1</sup>  and Babatunde Femi Bakare <sup>2</sup>

<sup>1</sup> Green Engineering Research Group, Department of Chemical Engineering, Faculty of Engineering and the Built Environment, Durban University of Technology, Steve Biko Campus, S4 Level 1, Durban 4000, South Africa; emmanuelk@dut.ac.za (E.K.T.); rathilals@dut.ac.za (S.R.)

<sup>2</sup> Environmental Pollution and Remediation Research Group, Department of Chemical Engineering, Mangosuthu University of Technology, Durban P.O. Box 12363, Durban 4026, South Africa; bfemi@mut.ac.za

\* Correspondence: 21450515@dut4life.ac.za

**Abstract:** Conventional anaerobic digestion is currently challenged by limited degradability and low methane production. Herein, it is proposed that magnetic nanoparticles (Fe<sub>3</sub>O<sub>4</sub>-NPs) and bioelectrochemical systems can be employed for the improvement of organic content degradation. In this study, the effect of electrode configuration was examined through the application of a bioelectrochemical system and Fe<sub>3</sub>O<sub>4</sub>-NPs in anaerobic digestion (AD). A microbial electrolysis cell with cylindrical electrodes (MECC) and a microbial electrolysis cell (MEC) with rectangular electrodes were compared against the traditional AD process. Biochemical methane potential (BMP) tests were carried out using digesters with a working volume of 800 mL charged with 300 mL inoculum, 500 mL substrate, and 1 g Fe<sub>3</sub>O<sub>4</sub>-NPs. The electrodes (zinc and copper) of both digesters were inserted inside the BMPs and were powered with 0.4 V for 30 days at 40 °C. The MECC performed better, improving degradability, with enhanced methane percentage (by 49% > 39.1% of the control), and reduced water pollutants (chemical-oxygen demand, total organic carbon, total suspended solids, turbidity, and color) by more than 88.6%. The maximum current density was 33.3 mA/m<sup>2</sup>, and the coulombic efficiency was 54.4%. The MECC showed a remarkable potential to maximize methane enhancement and pollution removal by adjusting the electrode configuration.

**Keywords:** bioelectrochemical; electrode configuration; anaerobic digestion; sewage sludge; magnetite nanoparticles (Fe<sub>3</sub>O<sub>4</sub>-NPs); mesophilic



**Citation:** Madondo, N.I.; Tetteh, E.K.; Rathilal, S.; Bakare, B.F. Application of Bioelectrochemical System and Magnetite Nanoparticles on the Anaerobic Digestion of Sewage Sludge: Effect of Electrode Configuration. *Catalysts* **2022**, *12*, 642. <https://doi.org/10.3390/catal12060642>

Academic Editors: Boxiong Shen and Peng Yuan

Received: 28 April 2022

Accepted: 9 June 2022

Published: 12 June 2022

**Publisher's Note:** MDPI stays neutral with regard to jurisdictional claims in published maps and institutional affiliations.



**Copyright:** © 2022 by the authors. Licensee MDPI, Basel, Switzerland. This article is an open access article distributed under the terms and conditions of the Creative Commons Attribution (CC BY) license (<https://creativecommons.org/licenses/by/4.0/>).

## 1. Introduction

The current over-reliance on non-renewable energy such as fossil fuels, the high levels of gas emissions, and the rise in fossil fuel prices have inspired researchers to look for other methods to generate sustainable energy. Rapid industrialization and over-population have also increased the generation of large quantities of waste, resulting in poor waste management and treatment processes, especially in developing nations [1,2]. The need for renewable energy to meet the ever-rising demand for energy and reduce reliance on fossil fuels is now becoming urgent [3]. There is likewise an ongoing quest for environmentally friendly and economical renewable energy technologies [4]. The anaerobic digestion process is an interesting renewable energy technology for converting biomass into biogas and degrading complex biochemical waste [5,6]. Biogas consists chiefly of methane (50%–75%), a valuable renewable energy source that may be used to substitute fossil fuels for energy generation [7–9]. The anaerobic digestion process is one of the most extensively used and cost-effective bioenergy recovery technologies worldwide. Despite its wide adoption, traditional anaerobic digestion is facing instability challenges as a result of substrate that is not balanced adequately for the availability

of electrons amongst different mechanism stages. This usually results in low biogas generation and a long digestion cycle [7,10,11].

The amount of sewage sludge produced in wastewater treatment plants is rising with the continuing expansion of wastewater networks, but also as a result of industrialization and high population growth [12]. Sewage sludge causes a sanitary threat as a result of its high concentrations of parasitic and pathogenic bacteria that have a negative impact when discharged into the environment [13]. Investigators and industries are currently looking for an alternative, potential, and competitive method for treating sewage sludge. The bioelectrochemical system is a promising method that has shown potential for stabilizing the electron transfer rates and improving the yield of methane in anaerobic digestion during shocks [14,15]. A bioelectrochemical system is an electrochemical technique wherein electroactive microorganisms (i.e., exoelectrogens) enhance the redox reactions at the outer layer of an electrode. This serves two purposes: (1) to eliminate biochemical matter, generating cleaner water that can be sent to surface waters; and (2) to generate renewable energy in the form of methane [16]. There are limited studies on the application of the bioelectrochemical system to improve the anaerobic digestion of sewage sludge. However, there is a basis for research that would support the effect of the bioelectrochemical system on sewage sludge treatment. Of late, it has been proven that the bioelectrochemical system affects some fluid properties, such as viscosity, polarization, electric charge, and surface tension. In the studies conducted so far, bioelectrochemical systems have primarily been employed for separating solids from wastewater, for example, waste-activated sludge [17,18].

Remarkably, recent findings have confirmed that the application of a bioelectrochemical system in anaerobic digestion improves microbial activity and electrochemical properties [19,20]. Despite this, the influence of the bioelectrochemical system on microbial metabolism still requires comprehensive study [21], particularly because proton and ion behavior in the bioelectrochemical system is not completely understood. As its superior electrochemical properties (such as current density) are likely to lead to significant methane generation, a limited number of investigations have studied the autotrophic pathway and heterotrophic pathway in this system.

The utilization of metal-based conductive supplements, such as magnetite nanoparticles ( $\text{Fe}_3\text{O}_4$ -NPs), in anaerobic digestion, can help enhance the hydrogenotrophic/volatile fatty acid interspecies electron transfer [22–25]. Interestingly, the synergistic effect of conductive supplements and the bioelectrochemical system can promote direct and indirect interspecies electron transfers [22]. In a study by Madondo et al. [19], the effect of adding  $\text{Fe}_3\text{O}_4$ -NPs to a bioelectrochemical system was investigated, and four digesters were compared: microbial fuel cell (MFC), microbial electrolysis cell (MEC), MEC with  $\text{Fe}_3\text{O}_4$ -NPs, and a control with no electrodes. The combination of 1 g  $\text{Fe}_3\text{O}_4$ -NPs and a bioelectrochemical system improved the efficiency of the biochemical degradation of biochemical substrate in anaerobic digestion. The outcome of the study also revealed a high methane percentage of 79.1% (which was 43% more than that of a traditional anaerobic digestion process), and contaminant removal of over 81.9% on carbon oxygen demand (COD), total organic carbon (TOC), total suspended solids (TSS), turbidity, and color. The use of MEC with  $\text{Fe}_3\text{O}_4$ -NPs improved biogas production by more than three times over that of the MEC digester. In terms of electrochemical efficiencies, the MEC with  $\text{Fe}_3\text{O}_4$ -NPs revealed greater electrical conductivity and the digester had the highest maximum current density ( $25 \text{ mA/m}^2$ ), which was about 3.3 times the maximum current density of an MFC ( $7.5 \text{ mA/m}^2$ ). This study was conducted at a mesophilic temperature of  $40^\circ\text{C}$  for a duration of 25 days. The design of the electrode is crucial for the treatment performance of organic substances in the bioelectrochemical system [20,26]. Even so, no study has been conducted on the configuration of electrodes in the synergistic interaction of  $\text{Fe}_3\text{O}_4$ -NPs and bioelectrochemical systems.

Therefore, this study focused on investigating the effect of electrode configuration through the application of a bioelectrochemical system and magnetite nanoparticles in the anaerobic digestion of sewage sludge. A bioelectrochemical system with rectangular electrodes (MEC) and a bioelectrochemical system with cylindrical electrodes (MECC)

were compared against a control digester with no electrodes. Parameters of interest were bioelectrochemical methane generation, stability indicator, electrochemical efficiencies, and pollutant removal.

## 2. Results and Discussions

### 2.1. Biogas Production and Methane Composition

In anaerobic digestion, the biogas accumulation graph is an important curve, as it shows the bacterial growth rate. Figure 1 portrays a graph of the biogas accumulation of MECC, MEC, and the control over a hydraulic retention time of 30 days. What can be seen from the graph is that all biogas accumulation curves had the shape of a sigmoidal curve (i.e., s-shape) while portraying three types of growth stages, namely lag phase, exponential growth phase, and steady-state phase. The lag phase is the initial stage in bacterial growth, in which microorganisms are still adapting to the new conditions, and therefore are not generating biogas. The MECC had the shortest lag phase, which suggested that the electroactive microorganisms were able to quickly adapt and accumulate on the surfaces of the electrodes. As for MEC and the control, their lag phases were higher, with the control exhibiting the longest lag phase (between 2 and 3 days). The digesters then reached the exponential growth phase, in which there was exponential growth of the bacterial community and exponential generation of biogas. All digesters then reached the steady-state phase, where biogas ceased production. Ultimately, the digester with the shortest lag phase (MECC) produced the highest accumulation of biogas of 14.5 mL (or 551.2 mL/g VS<sub>fed</sub>), which was 3.2 times the 4.6 mL (169.1 mL/g VS<sub>fed</sub>) biogas production of the control. Thus, the outcome of the study revealed that the use of a biochemical system reduces the lag phase, and a bioelectrochemical system with cylindrical electrodes shows faster microbial adaptation, which results in higher biogas production.

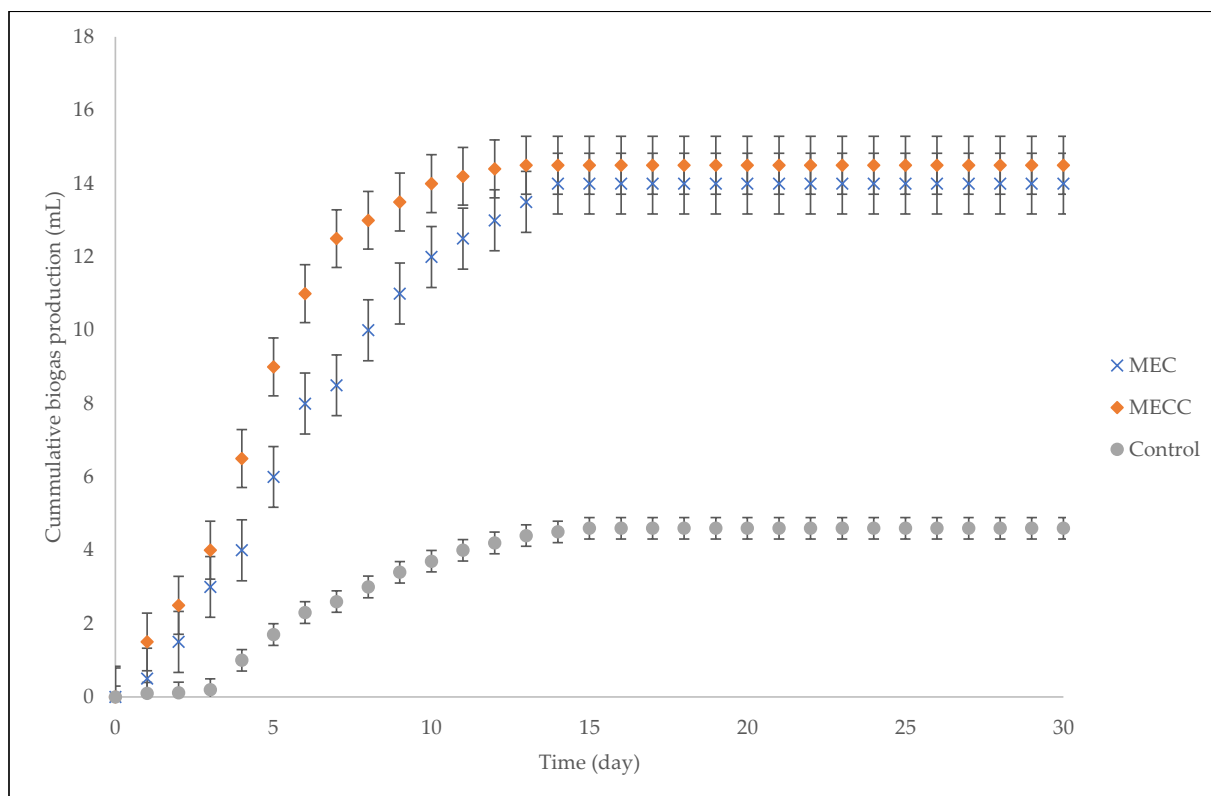
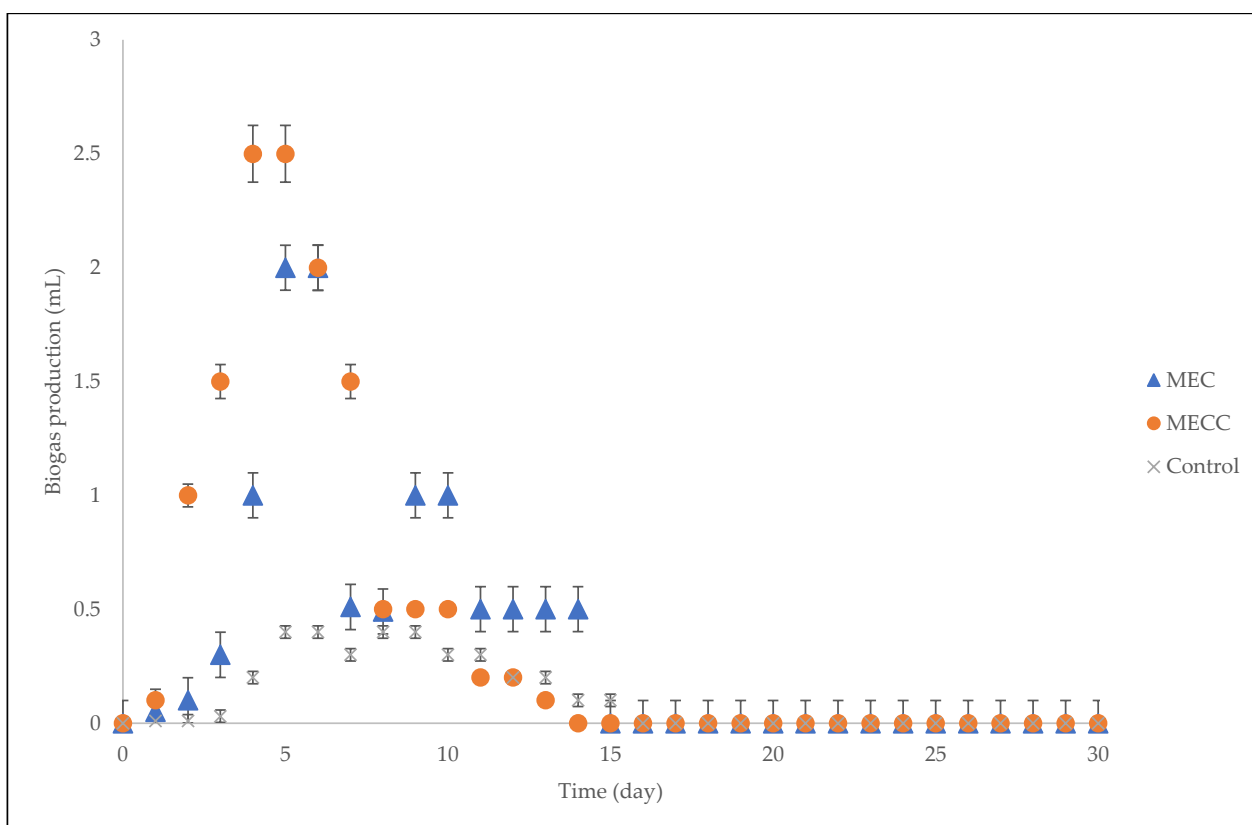


Figure 1. Cumulative biogas production.

Figure 2 shows the biogas production of the digesters daily. After passing the lag phase, the digesters reached the exponential growth stage. During the exponential growth

phase, the digesters firstly showed an exponential growth rate at an accelerating rate and then at a decelerating rate. Each digester then reached the inflection point, a point where curvature changes, i.e., from accelerating to decelerating. The MECC reached the inflection point earlier, followed by MEC and then lastly the control. The MECC had the greatest daily production of 2.5 mL (91.9 mL/g VS<sub>fed</sub>) on day 5. After passing the inflection point, the digesters showed a deceleration in biogas production. The digesters then reached the steady-state phase, where there was no biogas production. It is evident from the graph that all digesters ceased production after day 15.



**Figure 2.** Daily biogas production.

Although biogas production is important in anaerobic digestion, it is also important to investigate the efficiency of converting substrate to methane, i.e., content of methane in biogas and methane conversion rate (Table 1). Since the majority of metalloenzymes found in the path of biogas generation have many Fe<sub>2</sub>S<sub>2</sub>, Fe<sub>3</sub>S<sub>4</sub>, or Fe<sub>4</sub>S<sub>4</sub> clusters, iron is essential for cytochromes and CH<sub>4</sub> production [27–29]. The synergistic effects of iron-based nanoparticles (such as Fe<sub>3</sub>O<sub>4</sub>-NPS) and the bioelectrochemical system usually enhance methane generation by increasing the gas generation peak and improving the activities of metalloenzymes [19,29]. This is why the compositions of CH<sub>4</sub> in both the MEC (83.0%) and MECC (88.3%) were higher than in the control, with the MECC showing the greatest CH<sub>4</sub> increase of 49.1%. According to Oh et al. [15], the methane conversion rate that can be achieved from the traditional anaerobic digestion process does not accomplish its theoretical value of 350 mL/g COD<sub>removed</sub>. This is because the metabolic mechanisms cannot entirely transfer electrons from the substrate to CH<sub>4</sub> [30,31]. However, in this investigation, only the MECC had a value higher than the theoretical value (percentage improvement of >16.9%), which suggested that the electrode configuration of the MECC was able to assist the synergistic bioelectrochemical system and Fe<sub>3</sub>O<sub>4</sub>-NPs to completely transfer electrons thermodynamically from the substrate to CH<sub>4</sub>.

**Table 1.** Methane composition and methane conversion rate.

Digester Type	Methane (%)	Methane Conversion Rate (mL CH <sub>4</sub> /g COD <sub>removed</sub> )
MECC	88.2	409.2
MEC	83.0	337.4
Control	39.1	96.1

## 2.2. Electrochemical Characterization

Current density, heterotrophic methane yield, electrochemical methane yield, coulombic efficiency, electrical conductivity, and magnetic field were the electrochemical efficiencies that were measured for the bioelectrochemical systems. Current density, defined as the total electric current flowing across a unit cross-sectional area, is perhaps the most fundamental electrochemical measurement. Current density influences the electrochemical oxidation of a system since it controls the capability for active radical formation on the surface of the electrode [32]. It is evident from Figure 3 that current density increased in the early days of the digestion process. The rise in current density in the beginning took place because of microbial inoculation in the electrolytic liquid. For the same amount of voltage supplied (0.4 V), MECC reached its peak earlier than the MEC; MECC had the highest maximum current density of 33.3 mA/m<sup>2</sup> on day 5, whereas it took more days (11 days) for MEC to reach the maximum current density of 23.3 mA/m<sup>2</sup>. The MECC digester then stabilized on day 5, while MEC stabilized on day 11. This suggests that it took a shorter period for the electrochemically active microorganisms to be fully adapted and enriched on the electrodes of the MECC. The current or electric power could be optimized by trapping the microorganisms. A honeycomb or cylindrical structure has attractive characteristics for trapping microorganisms, which is why the microorganisms adapted faster to the MECC [33]. The decrease in the current density may take place because polymeric substances that occur outside cells can accumulate in the biological film over time [34]. Although the biogas generation graph (Figure 2) indicates that biogas ceased production after day 15, by contrast, the digesters showed a flow of electrons/current after these days (Figure 3). This denoted that biogas ceased production, but the only conversion that was taking place was CO<sub>2</sub> to CH<sub>4</sub>. Towards the end of the digestion period, current density suddenly fell, indicating a loss of electrons and hence the diminishing of methane. Current density then stabilized at a low current density after day 22 [35].

Even though the biochemical systems, both MECC and MEC, showed higher methane productions than the control, it is important to know the path that the methane took, i.e., the heterotrophic path (breaking down of complex matter) or the autotrophic path (generation of complex matter). The electrochemical methane yield and heterotrophic methane yield were fundamental parameters determining the path that the produced methane took (Figure 4). In general, an electrochemical methane yield that is above 100% denotes a higher COD to methane conversion rate. The electrochemical methane yield for MECC was 133.0%, that for MEC was 112.9%, and that for the control was 5.2%. Both biochemical systems had electrochemical methane yields greater than 100%, which implied that most of the methane produced took the heterotrophic path as opposed to the autotrophic path [36]. This was also confirmed by the fact that the contents of carbon dioxide in the bioelectrochemical systems (MECC = 11.8% and MEC = 17.0), were smaller than that in the control (60.9%) as well as higher heterotrophic methane yield (MECC = 72.3% and MEC = 44.6%), which further suggested the electrochemical reduction of carbon dioxide. The best-performing digester was the MECC, with the greatest electrochemical methane yield of 133.0%, the greatest heterotrophic methane yield of 72.3%, and the lowest carbon dioxide content of 11.8%, which denoted high conversion of carbon dioxide to methane, and hence, the heterotrophic pathway. On the other hand, the control revealed the lowest electrochemical methane yield, which suggested that the majority of the methane it produced took the autotrophic pathway, i.e., generation of complex matter.

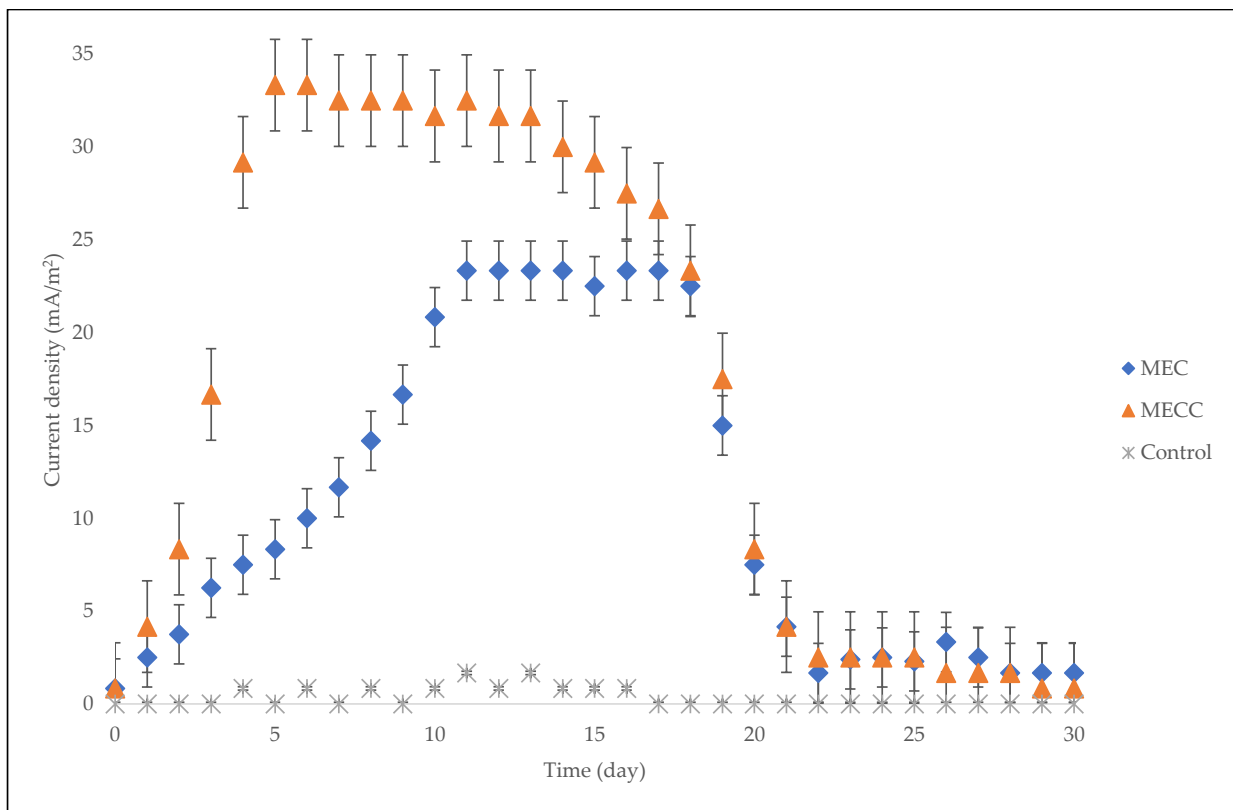


Figure 3. Effect of current density on digester type.

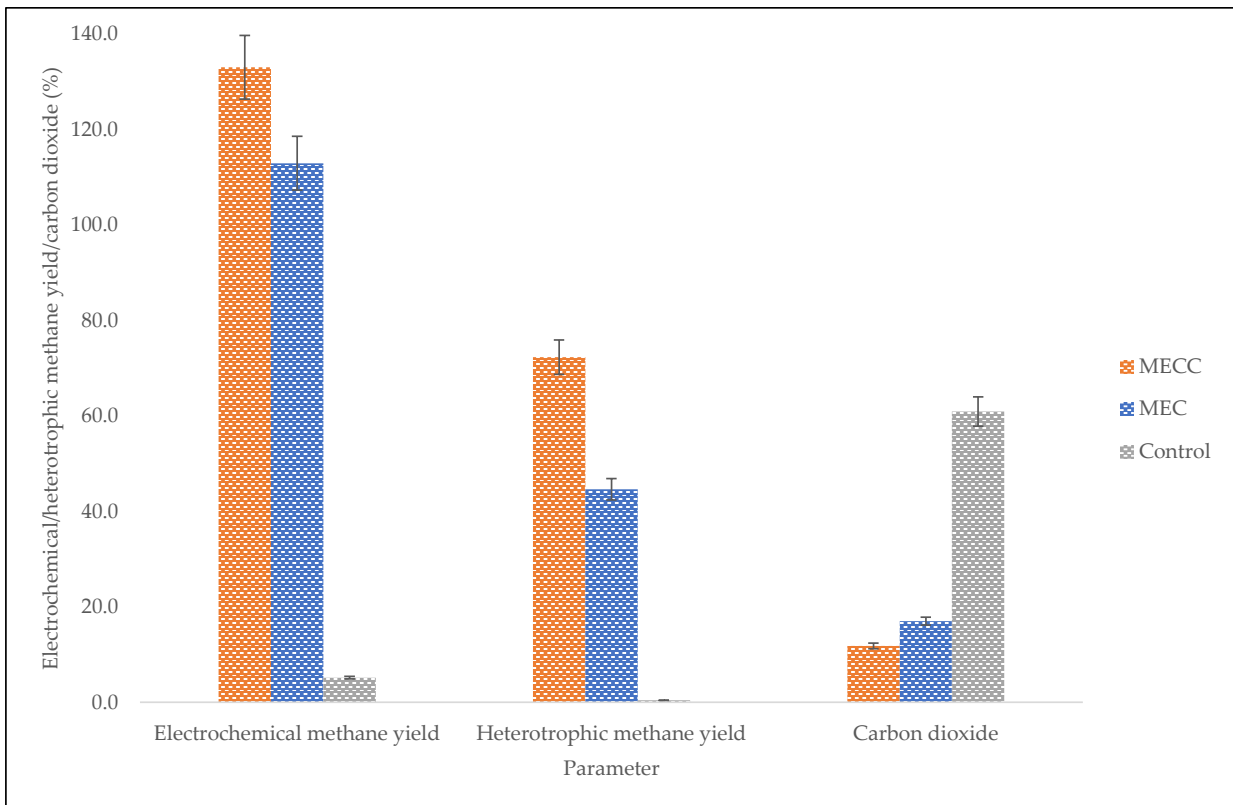
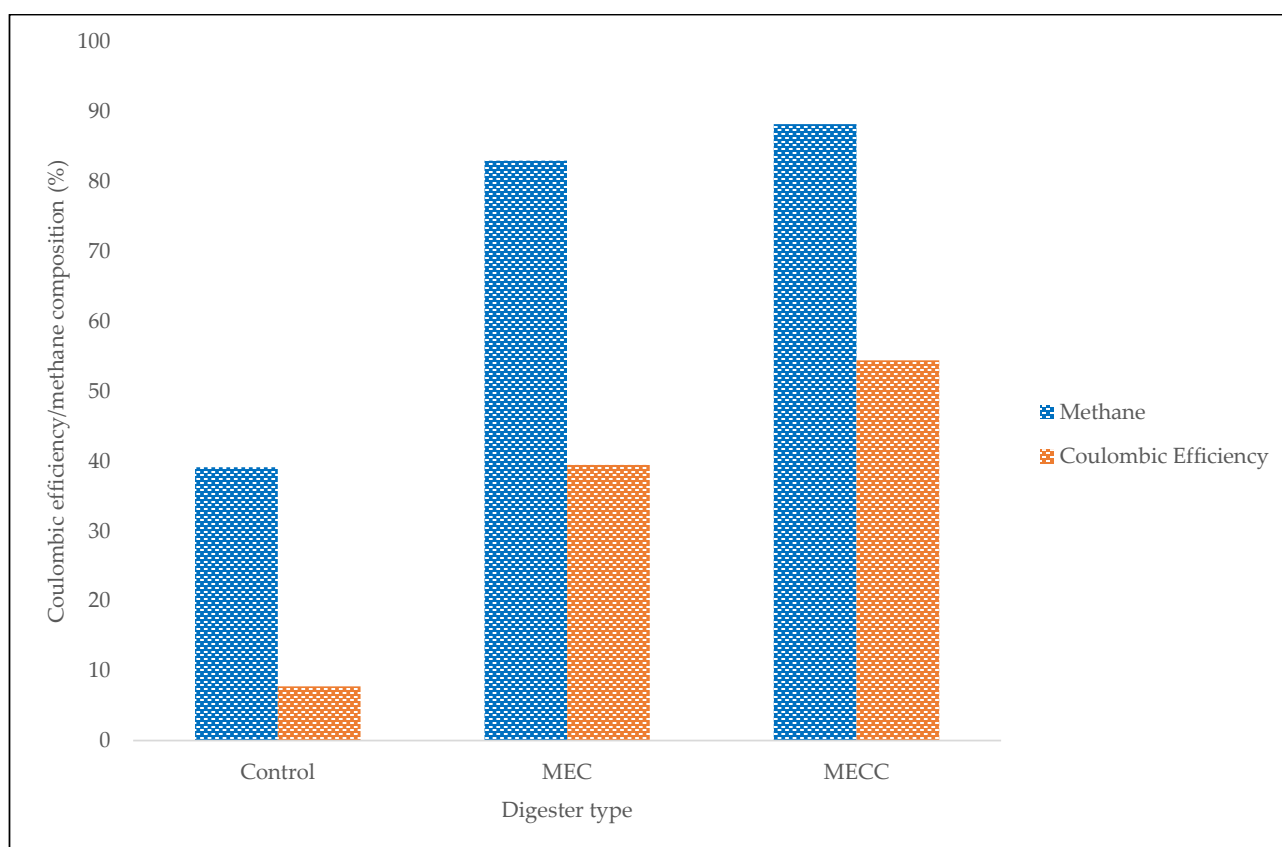


Figure 4. Electrochemical methane yield and heterotrophic methane yield with respect to carbon dioxide.

The coulombic efficiency is another important electrochemical characterization that governs the efficiency of a bioelectrochemical system. Coulombic efficiency is the percentage ratio between heterotrophic methane yield and electrochemical methane yield [5]. Basically, the coulombic efficiency denotes the amount of biochemical matter directly transformed into the current. In biochemical systems, higher coulombic efficiency values are desirable, as they signify higher biochemical matter to current conversion rates. Figure 5 presents coulombic efficiency and methane composition concerning digester type. The increasing order of the coulombic efficiencies depicts the following: MECC: 54.5% > MEC: 39.5% > control: 0% for methane compositions of 88.2%, 83.0%, and 39.1%, respectively. This suggests that an increase in coulombic efficiency was accompanied by an increase in methane composition. The greatest coulombic efficiency of 54.5% was achieved by the MECC, and this was due to the high methane content in the digester (88.2%) [37]. In addition to methane content, the coulombic efficiency is also influenced by ohmic losses, i.e., resistance that electrons and ions face as they move across a bioelectrochemical system. The higher the ohmic losses, the higher the resistance that electrons and ions experience, and hence, the lower the coulombic efficiency. Thus, the high coulombic efficiency of the MECC suggested that there were smaller ohmic losses in that system than in the other digesters. This means that the majority of electrons in the MECC took the heterotrophic pathway as opposed to the autotrophic pathway.



**Figure 5.** Coulombic efficiency and methane composition with respect to digester type.

On the other hand, the maximum current densities of 33.3, 23.3, and 0.1 mA/m<sup>2</sup> corresponded to coulombic efficiencies of 54.5% (MECC), 39.5% (MEC), and 0% (control), respectively. Therefore, an increase in current density enhanced coulombic efficiency.

Electrical conductivity is another helpful electrochemical efficiency that is able to detect electrical flow inside the digester as opposed to external electrical flow. Essentially, electrical conductivity represents the ability to conduct or transmit electrical current, and



the process must have thermodynamically satisfactory reactions and ion flow in the solution. Electrical conductivity ( $s$ ) is defined as:

$$s = \frac{j}{E} = \frac{1}{r} \quad (1)$$

where  $j$  represents current density and  $E$  is electric field intensity. The term  $r$  denotes resistivity. In a bioelectrochemical system, this denotes the resistance that electrons and ions face when they move across a bioelectrochemical system i.e., ohmic losses. Therefore from Equation (1), electrical conductivity is directly proportional to current density and inversely proportional to ohmic losses. This is why from Figure 6, an increase in maximum current density was accompanied by an increase in electrical conductivity. The digester with the highest electrical conductivity (293.0  $\mu\text{S}/\text{cm}$ ) was the MECC. The high electrical conductivity in the MECC certainly improved the way this digester performed, as it reduced the ohmic losses in the bioelectrochemical system [38]; the high concentration of electrons in the digester accelerated current flow in the exterior electrical circuit [39], which improved methane generation.

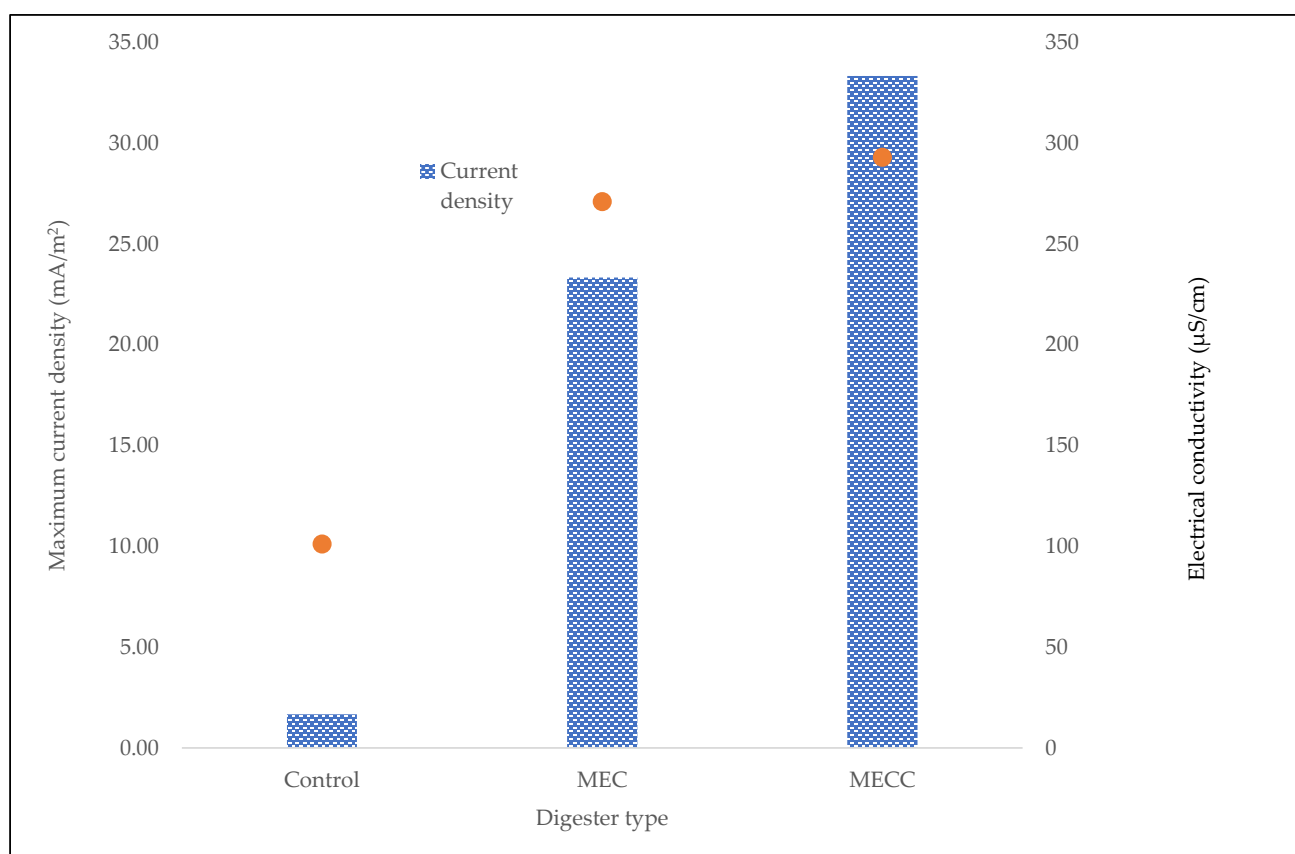


**Figure 6.** Influence of maximum current density on electrical conductivity.

The degree of impact exerted by a magnetic field or electromagnetism on the kinetics of the electrode mechanism is currently regarded as highly debatable. Based on Tafel data [40], electromagnetism has no substantial influence on the kinetics of the electrode mechanism; electromagnetism is achieved in magneto-impedance experimentations. Conversely, other studies have confirmed that exposure to high magnetic field strengths result in blockage of current density [24]. In this study, the current had a significant effect on electromagnetism; there was a direct relationship between current and magnetic field strength (Figure 7).



Biot-Savart's law also confirms that current is directly proportional to magnetic field, as shown in Equation (2):

$$B = \frac{\mu_0 NI}{2R} \quad (2)$$

where B is magnetic field intensity (T),  $\mu_0$  denotes permeability of free space (T.m/A), N is the number of turns, I is current density (A), and R is the radius (m). For the whole duration of the digestion period, the MECC had higher magnetic field strengths than both MEC and control, owing to the high current.

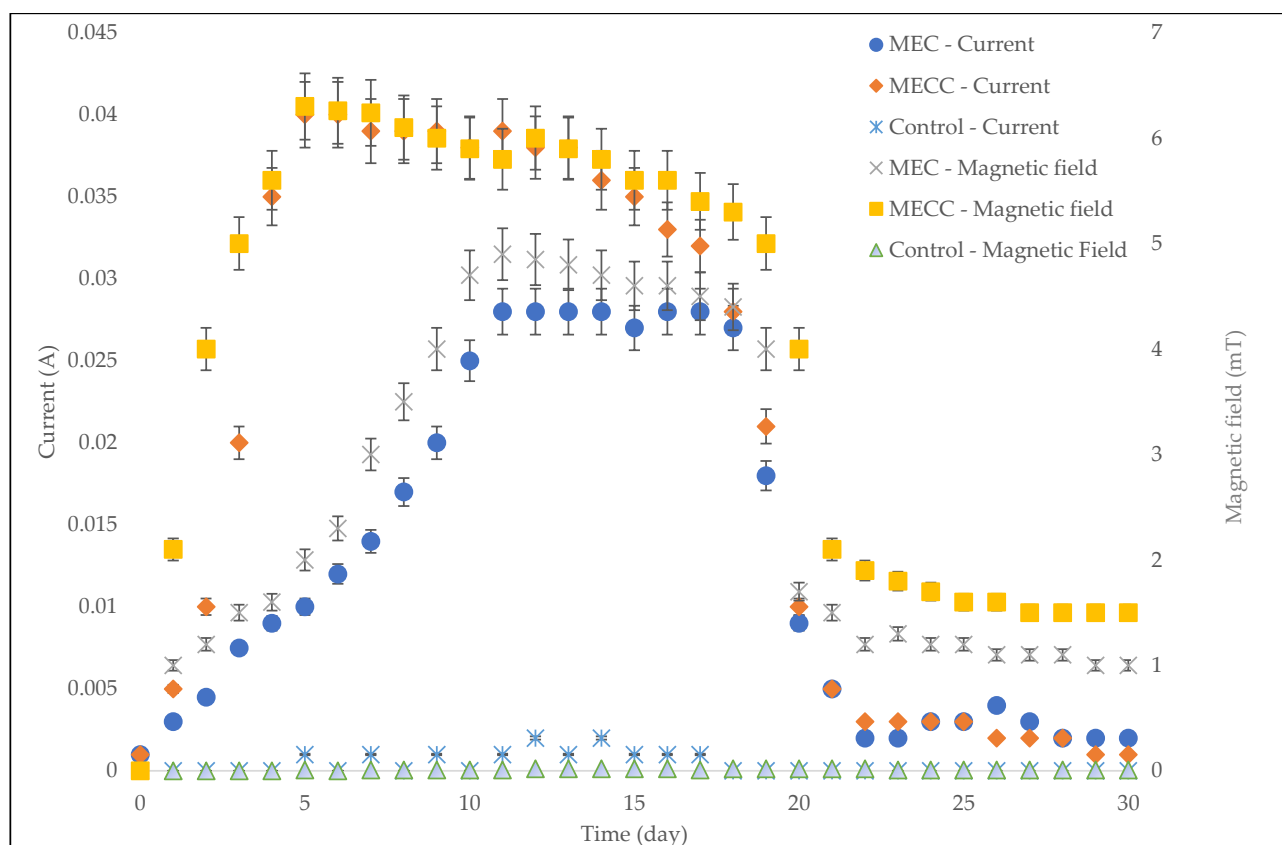


**Figure 7.** Effect of current on magnetic field.

### 2.3. Process Stability

In anaerobic digestion, the stability of the process can be obtained from the stable parameters of deterioration solution; for instance, pH. The pH of a solution in anaerobic digestion is vital since it influences bacterial growth and activity. Figure 8 depicts the effect of maximum current density on the pH of the digesters. The optimum pH for improving the electroactive acetogenins lies between 6.8 and 7.0, whereas for enhancing electroactive methanogens' performance, a pH in the range of 7.0 and 7.5 is required [36]. The digesters with a pH between 7.0 and 7.5 were MEC and MECC, which suggested that the synergistic bioelectrochemical system and  $\text{Fe}_3\text{O}_4$ -NPs helped to improve the electroactive methanogens' performance. The maximum current densities for the control, MEC, and MECC were 0.1, 23.3, and 33.3  $\text{mA}/\text{m}^2$ , whereas the pH values were 6.80, 7.26, and 7.50, respectively. Therefore, this result showed a direct proportion between maximum current density and pH. Halim et al. [35] also observed that for a pH range between 6.0 and 8.0, pH increased with an increase in current density.

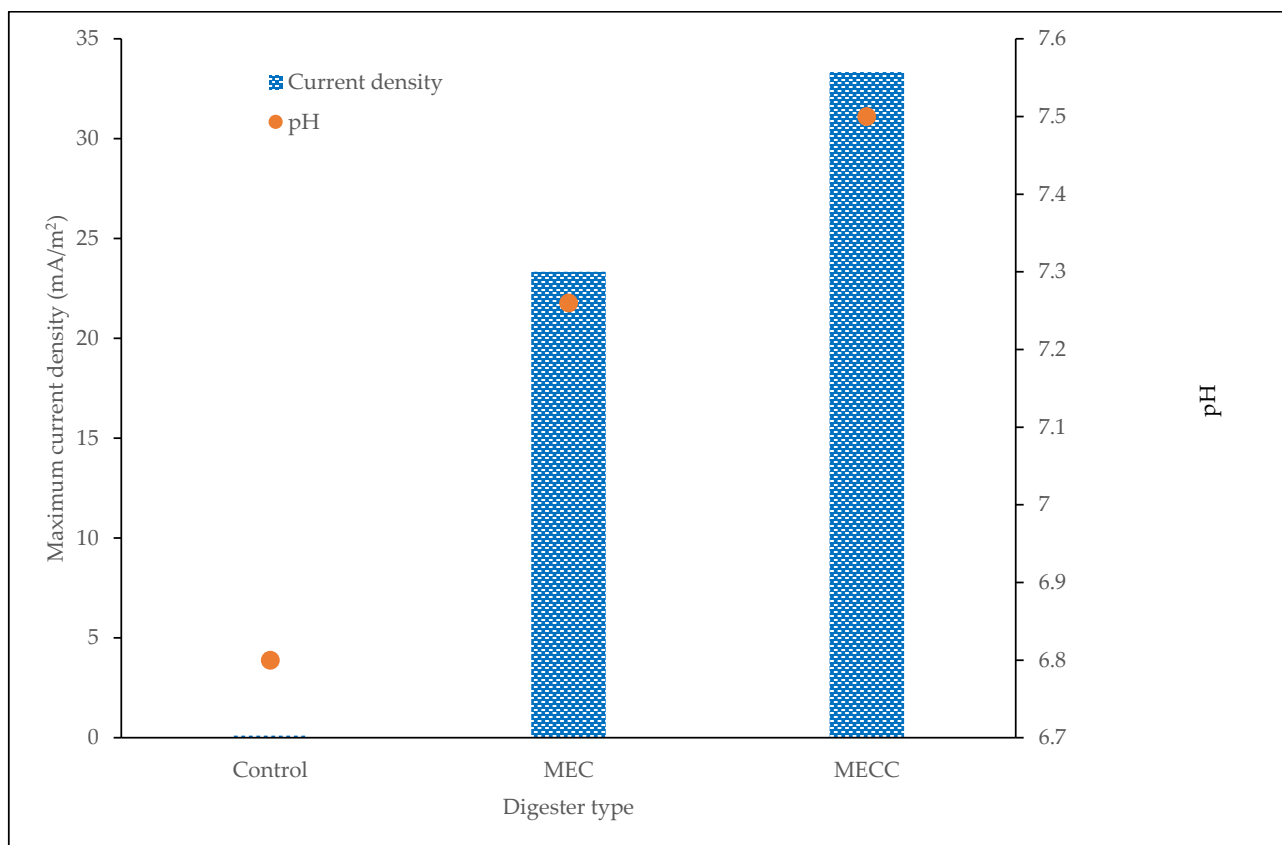


**Figure 8.** Effect of maximum current density on pH.

#### 2.4. Removal Efficiencies

Figure 9 shows the effect of electrode configuration on contaminants removed, namely: COD, TOC, TSS, turbidity, color, phosphate, and ammonia-nitrogen (NH<sub>3</sub>-N). The synergistic effects of Fe<sub>3</sub>O<sub>4</sub>-NPs and the bioelectrochemical systems, both MEC and MECC, showed higher contaminant removal than the control, with over 35.8% removal. Amongst the contaminants tested, COD had the highest treatability performance, and this was achieved by both MEC and MECC. This suggests that the synergistic effects of Fe<sub>3</sub>O<sub>4</sub>-NPs and the bioelectrochemical systems mostly improved the COD-to-gas conversion. This confirms the results obtained above in the electrochemical characterization section, where the high EMYs (above 100%) on both MEC and MECC indicated higher conversion rates of COD to methane. However, the best-performing digester was the MECC, with better water pollutant removal with COD (98.6%), TOC (95.9%), TSS (91.1%), turbidity (97.7%), and color (88.6%). In contrast, phosphate (76.3%) and NH<sub>3</sub>-N (43.7%) removal was better in the MEC. The current densities for MECC and MEC were 33.3 mA/m<sup>2</sup> and 23.3 mA/m<sup>2</sup>, whereas ammonia–nitrogen removal in each digester was 35.8% and 43.7%, respectively. This suggests that a decrease in current density increased ammonia–nitrogen removal. The same observation was found by Yao et al. [32], who observed that higher current densities resulted in low ammonia removal.

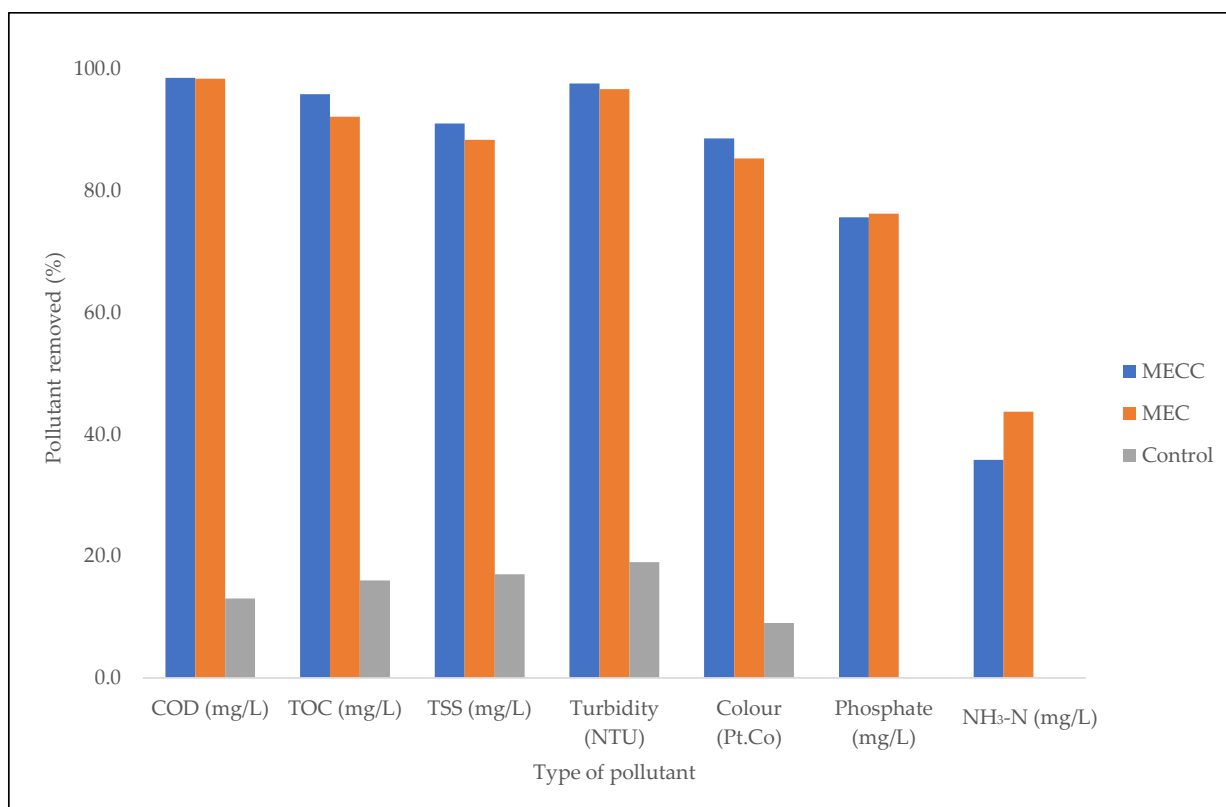


**Figure 9.** Effect of configuration on pollutant removal.

### 2.5. Kinetic Analysis

The modified Gompertz model was proposed for the evaluation of the performance of the anaerobic digestion of MECC, MEC and the control. Figure 10 shows the graphical representation of the modified Gompertz models and the measured biogas yields. From the graph, it is evident that the predicted biogas yield values were closer to the measured biogas yield values. This is more evident in Table 2, which depicts the predicted kinetic parameters for the modified Gompertz models. High  $R^2$  values were achieved for MECC (1.004), MEC (0.991), and the control (0.987), which suggested best fit with the operational data points. The  $R^2$  of the MECC was significantly higher than that of the other digesters, which indicated that the model of the MECC was more robust. On the other hand, the  $R^2$  of the control was the lowest, suggesting that the control had the most uneven biogas yields, and the modified Gompertz model was not able to significantly fit the operational data points. The production of biogas and the degradation rate rely on the hydrolysis constant rate ( $k$ ) [41]. The outcome of the results suggested a direct relationship between  $k$  and biogas yield, with the maximum biogas yield of 548.0 mL/g VS<sub>fed</sub> (MECC) obtained at the highest  $k$  value of 0.427/day. The maximum biogas yield was also higher for MECC (86.01 mL/g VS<sub>fed</sub>), which suggested the highest degradation rate. The lag phase ( $\lambda$ ) may be used to express the delayed response and adaptability of the microbes to the system. The higher  $\lambda$  value on the control could decrease the adaptability of microbes to the mechanism system and generate biogas over a long duration. The lag phase of the MECC (1.086 day) was lowest, which meant that the electroactive microorganisms were able to adapt faster in the MECC system than in the other digesters. The percentage difference between the maximum biogas yield potential and maximum biogas yield measured for MECC was zero, which further implied that the best fit model was the MECC.

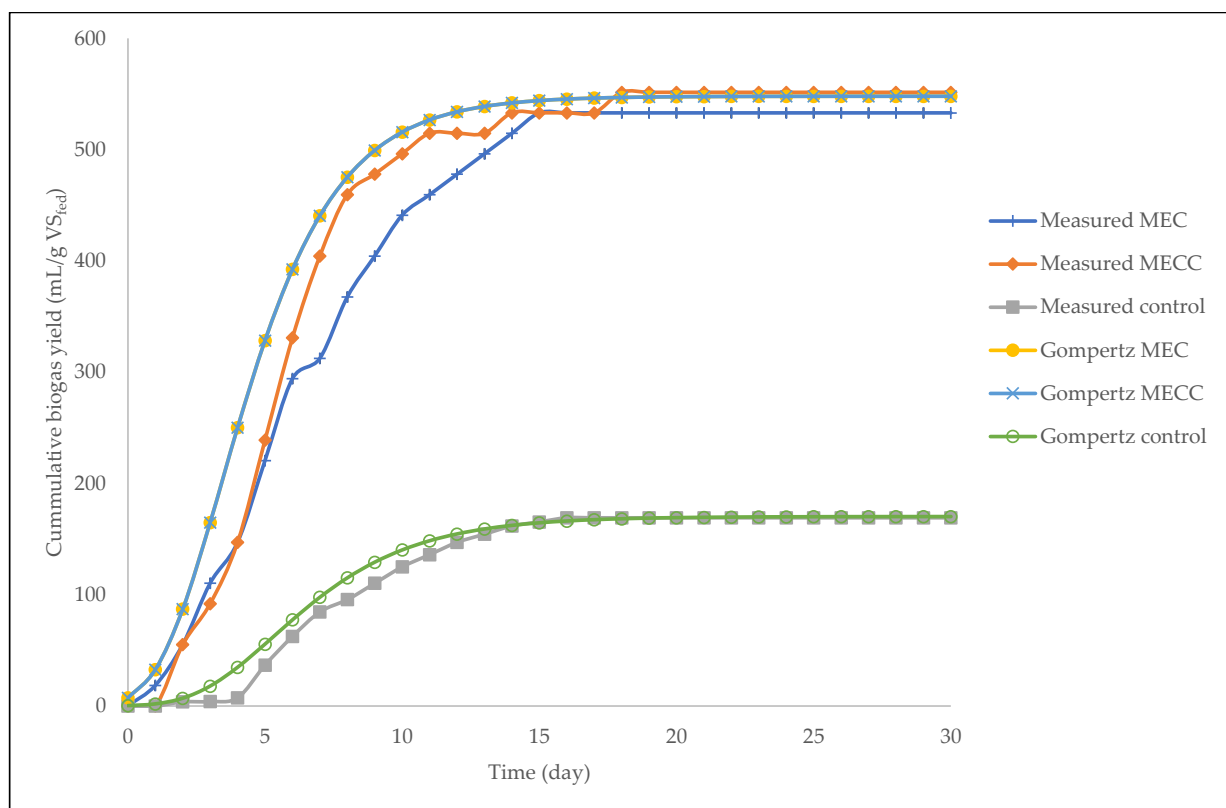


Figure 10. Cumulative biogas yield from the modified Gompertz model.

Table 2. Predicted kinetic parameters for the modified Gompertz models.

Parameter	Unit	MECC	MEC	Control
Coefficient of determination ( $R^2$ )	-	1.004	0.991	0.987
Constant rate ( $k$ )	1/day	0.427	0.350	0.306
Lag phase ( $\lambda$ )	day	1.086	1.425	2.469
Maximum biogas yield rate ( $B_m$ )	mL/g $VS_{fed}$ day	86.01	60.44	21.94
Maximum biogas potential ( $B_p$ )	mL/g $VS_{fed}$	548.0	537.7	170.2
Maximum biogas yield measured	mL/g $VS_{fed}$	548.0	537.0	170.0
Percentage difference	%	0.00	0.13	0.12

### 3. Materials and Methods

#### 3.1. Anaerobic Digester and Operation

The biochemical methane potential (BMP) tests were achieved using the following types of digesters: (1) microbial electrolysis cell (MEC): a digester with rectangular electrodes connected to a power supply, (2) microbial electrolysis cell with cylindrical electrodes (MECC), and (3) control: a digester with no electrodes/power supply (Figure 11). The digesters were Duran Schott bottles, with each digester consisting of an overall volume of 1 L (0.8 L working volume and 0.2 L headspace). Each digester was fed 0.3 L of sewage sludge for inoculation, 0.5 L of waste-activated sludge as a substrate, and 1 g of magnetite nanoparticles [19]. Each digester was enclosed with an airtight cap mounted at the top with four ports for liberating biogas to the gas collector through a 0.6 cm (inside diameter) silicone tubing, sampling, zinc electrode, and copper electrode. Both bioelectrochemical systems, MEC and MECC, were supplied with 0.4 V on the anode (zinc) and cathode (copper) electrodes (length: 12 cm, width: 1 cm). For the MECC, the configuration of the electrodes separated with silicone tubing strips (0.6 cm inside diameter) was rolled into a cylindrical form. The heating of the digesters was controlled via a circulating water bath

and the temperature inside each digester was kept at 40 °C for a duration of 30 days. To ensure homogeneity of the mixture, each digester was shaken by hand for one minute daily.

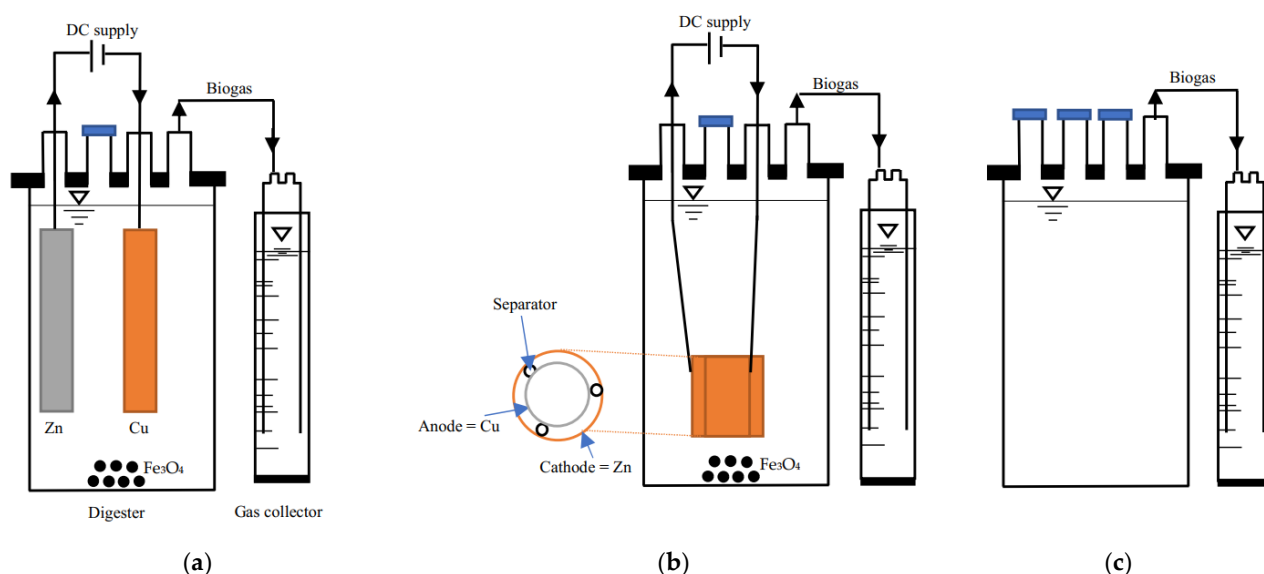


**Figure 11.** Drawing of anaerobic digestion: (a) rectangular microbial electrolysis cell (MEC); (b) cylindrical microbial electrolysis cell (MECC); and (c) control.

### 3.2. Magnetite Nanoparticle ( $Fe_3O_4$ -NPs) Preparation and Substrate/Reagents

The magnetite nanoparticles ( $Fe_3O_4$ -NPs) used in this investigation were taken from the  $Fe_3O_4$ -NPs synthesized by Amo-Duodu et al. [42] of the Green Engineering Research Group at Durban University of Technology, South Africa. The  $Fe_3O_4$ -NPs were synthesized via a co-precipitation method which involved the addition of chemical reagents, oleic acid, nickel (II) nitrate hexahydrate, sodium hydroxide, ferric chloride hexahydrate, and ferrous sulfate heptahydrate. The study included the analysis of  $Fe_3O_4$ -NPs morphological and physicochemical properties, which were examined by X-ray diffraction (XRD), Fourier-transform infrared spectroscopy (FTIR), and scanning electron microscopy/energy-dispersive X-ray (SEM/EDX). The XRD affirmed the crystal size (5.179 nm) and structure (face-centered cubic shape).

Inoculum (sewage sludge) and substrate (waste-activated sludge) originated from the municipal treatment company located in Durban, province of KwaZulu-Natal, South Africa. Both sewage sludge and waste-activated sludge were sampled using 20 L containers. The wastewater was homogenized and maintained under anaerobic conditions and kept at room temperature. For each digester, the digester was fed with sewage sludge and waste-activated sludge at a ratio of 0.3 L: 0.5 L. All chemical reagents were obtained from Labcare Supplies (PTY) LTD.

### 3.3. Analytical Methods and Calculations

A water displacement method was used to measure biogas production daily, whereas biogas composition was measured for methane and carbon dioxide using a gas analyzer (Geotech GA 5000). A Hanna H198129 conductivity meter was used to measure pH and electrical conductivity for the feed and effluent of wastewater. A digital Telsameter was used to determine the magnetic field strength. A Hach DR 3900 colorimeter (Hach, CO, USA) with standard reagents together with test kits, was used to measure the pollutant indicators: total solids (TSS), color, ammonia nitrogen ( $NH_3$ -N), total organic carbon (TOC), and chemical oxygen demand (COD). Characterization of the wastewater was evaluated using standard methods as proposed by APHA, Standard Methods for the Examination of Water and Wastewater [43]. A Hach 2100N turbidimeter was used to measure turbidity before and after digestion.

Equation (3) was used to determine the percentage of pollutant removed (PR):

$$\% \text{ PR} = \frac{\text{feed pollutant} - \text{effluent pollutant}}{\text{feed pollutant}} \times 100\% \quad (3)$$

A RMS multimeter (FLUKE 177 RMS, WA, USA) was used to measure cell voltage and current on a daily basis. Equations (4) and (5) were used to compute power density (P) and current density (j), respectively [44]:

$$P = jV \quad (4)$$

$$j = \frac{I}{A} \quad (5)$$

The symbol I denotes current (A), whereas A represents the electrode area (m<sup>2</sup>).

Equations (6) and (7) were used to calculate electrochemical methane yield and heterotrophic methane yield, respectively [36].

$$\text{Electrochemical methane yield} = \frac{\left[ \frac{V_C}{22.450} \right]}{\left[ \frac{M_O \int_{t=0}^t I \, dt}{e_O F} \right]} \times 100\% \quad (6)$$

$$\text{Heterotrophic methane yield} = \frac{\left[ \frac{V_C}{22.450} \right]}{\left[ \frac{V_I \Delta \text{COD}}{64} \right]} \times 100\% \quad (7)$$

The symbol  $V_C$  indicates the volume of methane (mL) generated and  $M_O$  is the molar mass of oxygen. The expression  $\int_{t=0}^t I \, dt$  represents the total number of electrons ( $e^-$ ). The term  $e_O (=4)$  is the quantity of  $e^-$  exchanged per mole of oxygen. The term  $F$  represents Faraday's constant (96.485 C/mol  $e^-$ ). The expression  $V_I$  symbolizes the volume of wastewater (mL). The term  $\Delta \text{COD}$  indicates the change in COD over time (t).

The coulombic efficiency (CE) of a bioelectrochemical system over time (t) was determined via Equation (8) [35,45,46]:

$$\text{CE} = \frac{M_O \int_{t=0}^t I \, dt}{e_O F V_I \Delta \text{COD}} \times 100\% \quad (8)$$

The modified Gompertz model was exercised to fit the cumulative biogas yield acquired from the investigational data points (Equation (9)).

$$M = B_p \times \exp \left\{ -\exp \left[ \frac{B_m \cdot e}{B_p} (\lambda - t) + 1 \right] \right\} = B_p \times [1 - \exp(-kt)] \quad (9)$$

where M is the biogas yield (mL/g VS<sub>fed</sub>),  $B_p$  is the maximum substrate biogas potential (mL/g VS<sub>fed</sub>),  $B_m$  is the maximum biogas yield rate (mL/g VS<sub>fed</sub>·day), e is a mathematical value otherwise known as Euler's number (2.7183),  $\lambda$  is the lag phase (days), t is the time (days), and k is the hydrolysis rate constant (1/day).

Table 3 shows characteristics of the feed before digestion.

**Table 3.** Characteristics of the feed.

Parameter	Quantity
pH	6.71 ± 0.52
Density (kg/m <sup>3</sup> )	1080.00 ± 29.10
Ammonia nitrogen (NH <sub>3</sub> -N, mg/L)	39.69 ± 2.77
Total organic carbon (TOC, mg/L)	3675.22 ± 48.23
Phosphate (mg/L)	9.74 ± 0.15
Total suspended solids (TSS, mg/L)	38.12 ± 1.35
Chemical oxygen demand (COD, mg/L)	2311.00 ± 199.57
Color (Pt.Co)	241.73 ± 5.29
Turbidity (NTU)	522.27 ± 7.86

#### 4. Conclusions

This paper focused on examining the influence of electrode configuration through the application of a bioelectrochemical system and Fe<sub>3</sub>O<sub>4</sub>-NPs on anaerobic digestion. Under the conditions applied, electrode configuration demonstrated a substantial effect on anaerobic digestion. The bioelectrochemical system that performed better in terms of bioelectrochemical methane generation, stability indicator, electrochemical efficiencies, and pollutant removal was the MECC. The MECC revealed better electrochemical efficiencies with coulombic efficiency (54.4%), maximum current density (33.3 mA/m<sup>2</sup>), and conductivity (293.0 μS/cm), which suggested that the system took the heterotrophic pathway. Furthermore, methane production was superior in the MECC, with a methane conversion rate of 409.2 mL CH<sub>4</sub>/g COD<sub>removed</sub> and methane content of 86%, values 313.1% and 49.1% greater than that of the control, respectively. Furthermore, the MECC showed better water pollutant removal: COD (98.6%), TOC (95.9%), TSS (91.1%), turbidity (97.7%), and color (88.6%). On the other hand, phosphates and ammonia–nitrogen were superior in the MEC, with 76.3% and 43.7% removal, respectively. In terms of kinetic tests, the modified Gompertz model of the MECC was the most appropriate model for fitting the accumulative biogas yield, with the best coefficient of determination (R<sup>2</sup>) of 1.004, highest hydrolysis constant rate (k) of 0.427/day, and lag phase (λ) of 1.086 days. Therefore, electrode configuration seems to be the key to improving the efficiency of the bioelectrochemical system, with the MECC demonstrating great potential to maximize methane generation and pollutant removal. Moreover, the outcomes of this research are of substantial interest for better comprehension of the synergism of the bioelectrochemical system and Fe<sub>3</sub>O<sub>4</sub>-NPs for methane generation, and recovery from anaerobic digestion digestate.

**Author Contributions:** Conceptualization, N.I.M., E.K.T. and S.R.; methodology, N.I.M.; validation, N.I.M.; investigation, N.I.M.; data curation, N.I.M.; writing—original draft preparation, N.I.M.; writing—review and editing S.R., B.F.B. and E.K.T.; administration, E.K.T.; supervision, S.R. and B.F.B. All authors have read and agreed to the published version of the manuscript.

**Funding:** This study was sponsored by the National Research Foundation (NRF), grant number 129076, Department of Chemical Engineering at Durban University of Technology.

**Data Availability Statement:** Not applicable.

**Acknowledgments:** The authors would like to thank the Green Engineering Research Group and Durban University of Technology.

**Conflicts of Interest:** The authors declare no conflict of interest.

#### References

1. Abdel-Shafy, H.I.; Mansour, M.S.M. Solid waste issue: Sources, composition, disposal, recycling, and valorization. *Egypt. J. Pet.* **2018**, *27*, 1275–1290. [[CrossRef](#)]
2. Ayeleru, O.O.; Olubambi, P.A. Chapter 13—Solid Waste Treatment Processes and Remedial Solution in the Developing Countries. In *Soft Computing Techniques in Solid Waste and Wastewater Management*; Elsevier: Amsterdam, The Netherlands, 2021; pp. 233–246. ISBN 9780128244630.



3. Gielen, D.; Boshell, F.; Saygin, D.; Bazilian, M.D.; Wagner, N.; Gorini, R. The role of renewable energy in the global energy transformation. *Energy Strategy Rev.* **2019**, *24*, 38–50. [[CrossRef](#)]
4. Bhatt, A.H.; Tao, L. Economic Perspectives of Biogas Production via Anaerobic Digestion. *Bioengineering* **2020**, *7*, 74. [[CrossRef](#)] [[PubMed](#)]
5. Madondo, N.I.; Chetty, M. Anaerobic co-digestion of sewage sludge and bio-based glycerol: Optimisation of process variables using one-factor-at-a-time (OFAT) and Box-Behnken Design (BBD) techniques. *S. Afr. J. Chem. Eng.* **2022**, *40*, 87–99. [[CrossRef](#)]
6. Kamperidou, V.; Terzopoulou, P. Anaerobic Digestion of Lignocellulosic Waste Materials. *Sustainability* **2021**, *13*, 12810. [[CrossRef](#)]
7. Kasinath, A.; Fudala-Ksiazek, S.; Szopinska, M.; Bylinski, H.; Artichowicz, W.; Remiszewska-Skwarek, A.; Luczkiewicz, A. Biomass in biogas production: Pretreatment and codigestion. *Renew. Sustain. Energy Rev.* **2021**, *150*, 111509. [[CrossRef](#)]
8. Cucchiella, F.; D'Adamo, I.; Gastaldi, M. Biomethane: A Renewable Resource as Vehicle Fuel. *Resources* **2017**, *6*, 58. [[CrossRef](#)]
9. Hassanein, A.; Witarsa, F.; Lansing, S.; Qiu, L.; Liang, Y. Bio-Electrochemical Enhancement of Hydrogen and Methane Production in a Combined Anaerobic Digester (AD) and Microbial Electrolysis Cell (MEC) from Dairy Manure. *Sustainability* **2020**, *12*, 8491. [[CrossRef](#)]
10. Guo, P.; Zhou, J.; Ma, R.; Yu, N.; Yuan, Y. Biogas Production and Heat Transfer Performance of a Multiphase Flow Digester. *Energies* **2019**, *12*, 1960. [[CrossRef](#)]
11. Pawar, A.A.; Karthic, A.; Lee, S.; Pandit, S.; Jung, S.P. Microbial electrolysis cells for electromethanogenesis: Materials, configurations and operations. *Environ. Eng. Res.* **2020**, *27*, 200484. [[CrossRef](#)]
12. Durđević, D.; Blecich, P.; Jurić, Ž. Energy Recovery from Sewage Sludge: The Case Study of Croatia. *Energies* **2019**, *12*, 1927. [[CrossRef](#)]
13. Rorat, A.; Courtois, P.; Vandenbulcke, F.; Lemiere, S. Sanitary and environmental aspects of sewage sludge management. In *Industrial and Municipal Sludge*; Butterworth-Heinemann: Oxford, UK, 2019; pp. 155–180. ISBN 9780128159071.
14. Park, J.; Jiang, D.; Lee, B.; Jun, H.B. Towards the practical application of bioelectrochemical anaerobic digestion (BEAD): In-sights into electrode materials, reactor configurations, and process designs. *Water Res.* **2020**, *184*, 116214. [[CrossRef](#)] [[PubMed](#)]
15. Oh, G.-G.; Song, Y.-C.; Bae, B.-U.; Lee, C.-Y. Electric Field-Driven Direct Interspecies Electron Transfer for Bioelectrochemical Methane Production from Fermentable and Non-Fermentable Substrates. *Processes* **2020**, *8*, 1293. [[CrossRef](#)]
16. Sleutels, T.H.J.A.; Molenaar, S.D.; Ter Heijne, A.; Buisman, C.J.N. Low Substrate Loading Limits Methanogenesis and Leads to High Coulombic Efficiency in Bioelectrochemical Systems. *Microorganisms* **2016**, *4*, 7. [[CrossRef](#)] [[PubMed](#)]
17. Debowski, M.; Zieliński, M. Technological Effectiveness of Sugar-Industry Effluent Methane Fermentation in a Fluidized Active Filling Reactor (FAF-R). *Energies* **2020**, *13*, 6626. [[CrossRef](#)]
18. Zielinski, M.; Debowski, M.; Krzemieniewski, M.; Dudek, M.; Grala, A. Effect of constant magnetic field with various values of magnetic induction on effectiveness of dairy wastewaters treatment under anaerobic conditions. *Pol. J. Environ. Stud.* **2014**, *23*, 255–261.
19. Madondo, N.I.; Tetteh, E.K.; Rathilal, S.; Bakare, B.F. Synergistic Effect of Magnetite and Bioelectrochemical Systems on Anaerobic Digestion. *Bioengineering* **2021**, *8*, 198. [[CrossRef](#)]
20. An, Z.; Feng, Q.; Zhao, R.; Wang, X. Bioelectrochemical Methane Production from Food Waste in Anaerobic Digestion Using a Carbon-Modified Copper Foam Electrode. *Processes* **2020**, *8*, 416. [[CrossRef](#)]
21. Zieliński, M.; Debowski, M.; Kazimierowicz, J. The Effect of Static Magnetic Field on Methanogenesis in the Anaerobic Digestion of Municipal Sewage Sludge. *Energies* **2021**, *14*, 590. [[CrossRef](#)]
22. Paritosh, K.; Yadav, M.; Chawade, A.; Sahoo, D.; Kesharwani, N.; Pareek, N.; Vivekanand, V. Additives as a Support Structure for Specific Biochemical Activity Boosts in Anaerobic Digestion: A Review. *Front. Energy Res.* **2020**, *8*, 88. [[CrossRef](#)]
23. Baek, G.; Kim, J.; Kim, S.; Lee, C. Role and Potential of Direct Interspecies Electron Transfer in Anaerobic Digestion. *Energies* **2018**, *11*, 107. [[CrossRef](#)]
24. Kumar, S.S.; Ghosh, P.; Kataria, N.; Kumar, D.; Thakur, S.; Pathania, D.; Kumar, V.; Nasrullah, M.; Singh, L. The role of conductive nanoparticles in anaerobic digestion: Mechanism, current status and future perspectives. *Chemosphere* **2021**, *280*, 130601. [[CrossRef](#)]
25. Yang, Z.; Guo, R.; Shi, X.; Wang, C.; Wang, L.; Dai, M. Magnetite nanoparticles enable a rapid conversion of volatile fatty acids to methane. *RSC Adv.* **2016**, *6*, 25662–25668. [[CrossRef](#)]
26. Dange, P.; Pandit, S.; Jadhav, D.; Shanmugam, P.; Gupta, P.K.; Kumar, S.; Kumar, M.; Yang, Y.H.; Bhatia, S.K. Recent Developments in Microbial Electrolysis Cell-Based Biohydrogen Production Utilizing Wastewater as a Feedstock. *Sustainability* **2021**, *13*, 8796. [[CrossRef](#)]
27. Paulo, L.M.; Stams, A.J.M.; Sousa, D.Z. Methanogens, sulphate and heavy metals: A complex system. *Rev. Environ. Sci. Bio/Technol.* **2015**, *14*, 537–553. [[CrossRef](#)]
28. Glass, J.B.; Orphan, V.J. Trace Metal Requirements for Microbial Enzymes Involved in the Production and Consumption of Methane and Nitrous Oxide. *Front. Microbiol.* **2012**, *3*, 61. [[CrossRef](#)]
29. Zhang, J.; Lu, T.; Wang, Z.; Wang, Y.; Zhong, H.; Shen, P.; Wei, Y. Effects of magnetite on anaerobic digestion of swine manure: Attention to methane production and fate of antibiotic resistance genes. *Bioresour. Technol.* **2019**, *291*, 121847. [[CrossRef](#)]
30. Feng, Q.; Song, Y.-C.; Ahn, Y. Electroactive microorganisms in bulk solution contribute significantly to methane production in bioelectrochemical anaerobic reactor. *Bioresour. Technol.* **2018**, *259*, 119–127. [[CrossRef](#)]

31. Shen, L.; Zhao, Q.; Wu, X.; Li, X.; Li, Q.; Wang, Y. Interspecies electron transfer in syntrophic methanogenic consortia: From cultures to bioreactors. *Renew. Sustain. Energy Rev.* **2015**, *54*, 1358–1367. [[CrossRef](#)]
32. Yao, J.; Mei, Y.; Xia, G.; Lu, Y.; Xu, D.; Sun, N.; Wang, J.; Chen, J. Process Optimization of Electrochemical Oxidation of Ammonia to Nitrogen for Actual Dyeing Wastewater Treatment. *Int. J. Environ. Res. Public Heal.* **2019**, *16*, 2931. [[CrossRef](#)]
33. Tokonami, S.; Kurita, S.; Yoshikawa, R.; Sakurai, K.; Suehiro, T.; Yamamoto, Y.; Tamura, M.; Karthaus, O.; Iida, T. Light-induced assembly of living bacteria with honeycomb substrate. *Sci. Adv.* **2020**, *6*, eaaz5757. [[CrossRef](#)] [[PubMed](#)]
34. Zhang, L.; Zhu, X.; Li, J.; Liao, Q.; Ye, D. Biofilm formation and electricity generation of a microbial fuel cell started up under different external resistances. *J. Power Sources* **2011**, *196*, 6029–6035. [[CrossRef](#)]
35. Halim, A.; Rahman, O.; Ibrahim, M.; Kundu, R.; Biswas, B.K. Effect of Anolyte pH on the Performance of a Dual-Chambered Microbial Fuel Cell Operated with Different Biomass Feed. *J. Chem.* **2021**, *2021*, 5465680. [[CrossRef](#)]
36. Nelabhotla, A.B.T.; Dinamarca, C. Bioelectrochemical CO<sub>2</sub> Reduction to Methane: MES Integration in Biogas Production Processes. *Appl. Sci.* **2019**, *9*, 1056. [[CrossRef](#)]
37. Villano, M.; Aulenta, F.; Ciucci, C.; Ferri, T.; Giuliano, A.; Majone, M. Bioelectrochemical reduction of CO<sub>2</sub> to CH<sub>4</sub> via direct and indirect extracellular electron transfer by a hydrogenophilic methanogenic culture. *Bioresour. Technol.* **2010**, *101*, 3085–3090. [[CrossRef](#)] [[PubMed](#)]
38. Moreno, M.C. Anaerobic Digestion and Bioelectrochemical Systems Combination for Energy and Nitrogen Recovery Optimization. Ph.D. Thesis, The Polytechnic University of Catalonia, Barcelona, Spain, 2016.
39. Hamed, M.S.; Majdi, H.S.; Hasan, B.O. Effect of Electrode Material and Hydrodynamics on the Produced Current in Double Chamber Microbial Fuel Cells. *ACS Omega* **2020**, *5*, 10339–10348. [[CrossRef](#)]
40. Chopart, J.-P.; Douglade, J.; Fricoteaux, P.; Olivier, A. Electrodeposition and electrodisolution of copper with a magnetic field: Dynamic and stationary investigations. *Electrochim. Acta* **1991**, *36*, 459–463. [[CrossRef](#)]
41. Mao, C.; Wang, X.; Xi, J.; Feng, Y.; Ren, G. Linkage of kinetic parameters with process parameters and operational conditions during anaerobic digestion. *Energy* **2017**, *135*, 352–360. [[CrossRef](#)]
42. Amo-Duodu, G.; Tetteh, E.K.; Rathilal, S.; Chollom, M. Synthesis and characterization of magnetic nanoparticles: Biocatalytic effects on wastewater treatment. *Mater. Today Proc.* **2022**, *in press*. [[CrossRef](#)]
43. APHA; AWWA; WEF. *Standard Methods for Examination of Water and Wastewater*, 22nd ed.; American Public Health Association: Washington, WA, USA, 2012.
44. Wang, M.; Yan, Z.; Huang, B.; Zhao, J.; Liu, R. Electricity Generation by Microbial Fuel Cells Fuelled with Enteromorpha Prolifera Hydrolysis. *Int. J. Electrochem. Sci.* **2013**, *8*, 2104–2111.
45. Nandy, A.; Kumar, V.; Mondal, S.; Dutta, K.; Salah, M.; Kundu, P.P. Performance evaluation of microbial fuel cells: Effect of varying electrode configuration and presence of a membrane electrode assembly. *New Biotechnol.* **2015**, *32*, 272–281. [[CrossRef](#)] [[PubMed](#)]
46. Madondo, N.I.; Kweinor Tetteh, E.; Rathilal, S.; Bakare, B.F. Effect of an Electromagnetic Field on Anaerobic Digestion: Comparing an Electromagnetic System (ES), a Microbial Electrolysis System (MEC), and a Control with No External Force. *Molecules* **2022**, *27*, 3372. [[CrossRef](#)] [[PubMed](#)]